A Filter-Antenna with Reflector Based on Metamaterials for Railway Applications

Wyssem Fathallah[1,*], Taoufik Aguili[1]

[1]Research Lab LR-99-ES21, University El Manar, Tunisia

Abstract

This study examines the effectiveness of a band-pass filter integrated with an antenna to reduce electromagnetic interference (EMI) in railway wireless systems. The proposed structure consists of a planar metamaterial screen mapped onto a rectangular dielectric surface, integrated at a short distance from a patch radiating element operating at 5.9 GHz. This configuration preserves both the return loss and radiation pattern characteristics of the patch antenna. within the desired frequency band while effectively reflecting interference signals outside of the band. Additionally, it offers the benefits of a compact, low-profile design. Our contribution consists of designing a bandpass filter operating at a frequency of 5.9 GHz, dedicated to railway transportation, exhibiting high selectivity at low frequencies where multiple signals are utilized.We design a reflector based on FSS (Frequency Selective Surface) to enhance the antenna's gain. and have better directivity of the proposed antenna.

Keywords

Antenna, Electromagnetic Interference, Enhancement gain, Metamaterial, Railways

1. Introduction

Electromagnetic Interference (EMI) poses a threat to the functionality of electronic devices, equipment, and systems employed in vital transmission contexts like aerospace, military, and medical electronics, as well as navigation, vehicle control, and public transportation systems. The causes of electromagnetic interference are numerous, encompassing both natural and artificial sources. The consequences may vary from transient disturbances and data compromises to complete system breakdowns and, in extreme cases, loss of life [1].

For engineers, it's crucial to acknowledge how electromagnetic energy within the operating environment can induce interference. Absent this fundamental comprehension of electromagnetic interference, you may design joints lacking adequate protection against electromagnetic fields in the spectrum between 3 kHz and 300 GHz. In general, Electromagnetic interference sources can be categorized broadly into ambient electromagnetic interference and power quality issues. Railway and public transportation systems encounter unique challenges stemming from factors like emissions from train control and propulsion systems, high-voltage contact communication, third rails, and train signaling and control systems. Indeed, multiple antennas have to be installed on the rooftop to support the 900MHz and 1900MHz bands to ensure reception diversity as well as multiplexing gains leveraging Multiple Input Multiple Output (MIMO) techniques. However, the presence of numerous antenna in a limited space causes interference which harms the performance of the throughput of the system. Indeed, for antennas that share a common ground plane, the isolation can be low. This will cause a degradation in the antennas efficiency. Accordingly, antenna isolation is a technique for separating antennas that coexist so that there is only acceptable levels of interference between systems. It is a challenging task as antenna to antenna isolation is a measure of how are the antennas coupled. In this paper, we limit our study to the railway transportation system. In this system, low-frequency, high-power signals can also interfere with high-frequency wireless communications. Indeed, on a railway track, a train communicates at all

WAISS'2024: 1st Euro-Mediterranean Workshop on Artificial Intelligence and Smart Systems, October 15, 2024, Djerba, Tunisia (Co-located with the 17th International Conference on Verification and Evaluation of Computer and Communication Systems (VECoS'2024), October 15-18, 2024, Djerba, Tunisia)

*Corresponding author.

fathallahwyssem@gmail.com (W. Fathallah); taoufik.aguili@gmail.com (T. Aguili)

0009-0008-6316-5829 (W. Fathallah); 0000-0001-5071-013X (T. Aguili)

times, and the presence of communication systems of any wavelength can interact with the train and cause issues. This is why there is a need for materials capable of blocking or filtering waves to prevent reactions with undesirable fields. Our contribution consists of designing a bandpass filter operating at a frequency of 5.9 GHz, dedicated to railway transportation, exhibiting high selectivity at low frequencies where multiple signals are utilized. It will serve as electromagnetic shielding in the low-frequency range. This filter will be designed with miniature periodic cells of the "Frequency Selective Surface" (FSS) type placed above the antenna and very close to it (at a distance $e_1 = \frac{\lambda}{2}$. It should not disturb the distribution of the electromagnetic field in the near field and far field, while maintaining the dual polarization of the antenna (TE and TM). Additionally, it should not be highly sensitive to the angle of the incident wave.

Frequency Selective Surfaces have been extensively researched and have received significant focus in the development of antennas, radars, and electromagnetic compatibility within the microwave and millimeter-wave frequency ranges for many years. They have been proposed for use as spatial filters [1], radar cross-section (RCS) reflectors [2], and in the design of multiple-frequency antennas.

FSS structures are often periodic and flat.They may comprise metallic elements with various shapes or apertures carved into a metal plate arranged in a regular pattern within a two-dimensional array. The primary attribute of an FSS is its ability to be nearly transparent in a given frequency range and to effectively reflect electromagnetic fields (EM) outside of that interval, there by providing electromagnetic shielding and exhibiting filtering properties. The collective frequency behavior of the structure, including its transfer function, bandwidth, and polarization, is determined by the type and geometry of the elements, spacing between the elements, spatial periods, substrate parameters, and the presence or absence of cascading layers in an FSS.

A notable feature of FSS is that the size of the unit cells is less than half a wavelength. Frequency-selective properties result from mutual interactions of the elements, requiring a large number of unit cells to observe the desired frequency-selective behavior. On the other hand, for certain applications, insensitivity to the angle of incidence of the exciting incident wave is required. Consequently, the screen size must be small. To achieve a compromise, FSS with miniature elements have been proposed [3] -[7]. This trait endows FSS with high-order frequency responses that demonstrate minimal sensitivity to the angle of incidence. These spatial filters maintain effective operation even when positioned at distances close to approximately one-tenth of the antenna's wavelength. Cascading FSS layers further augment the frequency response of these filters [8]. However, there are limited studies that have designed the integration of antennas and FSS. The coupling between the miniaturization of FSS and the patch antenna array, which is angle-insensitive and provides higher-order spatial filtering, is discussed in [7]. A combined filter-antenna setup, comprising a conical FSS radome and a monopole antenna, has been successfully implemented in [9]-[17].

2. Design Methodology of a Miniature FSS-Based Filter

We present a configuration illustrated in Figures 1 and 2, featuring symmetry concerning the primary polarization axes and demonstrating identical equivalent circuitry for both horizontal and vertical polarization. This assembly can be conveniently produced by depositing components on opposing sides of a dielectric substrate. Our proposed design employs Rogers RT 5880 as the substrate, with dimensions $h = 0.254, mm$, permittivity of 2.2, and a loss coefficient of 0.0009. On one side, a circular metal patch of radius R is etched, while on the other side, a square metal frame with side length D and a metal line width W is present. The period of this square cell is D.

Our aim is to reduce the dimensions D of the cell while targeting a specific resonance frequency. We establish the condition $D < \frac{\lambda}{2}$, where λ denotes the wavelength, with the resonance frequency controlled by adjusting parameters r and W. The geometrical attributes of the depicted FSS cell in Figure 1 are fine-tuned to resonate at 5.9 GHz, with detailed values listed in Table 1.

Figures 3-6 present simulation outcomes of the S parameters for the proposed structure in Figures 1 and 2 under TE and TM modes across various angles of incidence θ. Notably, the FSS structure,

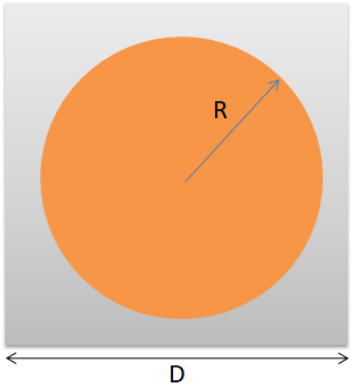

Figure 1: Front view of FSS filter.

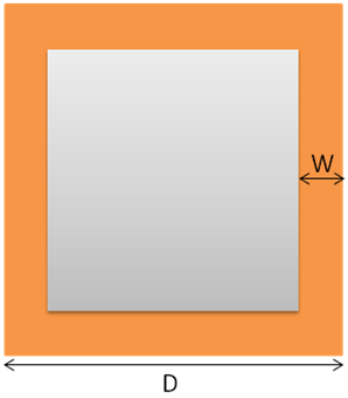

Figure 2: Back view of FSS filter.

Table 1
GEOMETRIC PARAMETERS OF THE PROPOSED FSS CELL OPTIMIZED AT 5.9 GHz.

Parameters	D	W	R
Values (mm)	12	1.4	5.45

resonating at 5.9 GHz, demonstrates a $-3\,dB$ bandwidth spanning 0.77 GHz in TE mode (equivalent to 13% of the bandwidth fraction) with an insertion loss of $-0.20\,dB$ at 5.9 GHz for normal incidence and $-0.33\,dB$ for an incidence angle of 40°. In TM mode, the insertion loss varies from $-0.20\,dB$ to $-0.22\,dB$ as the incidence angle escalates from 0° to 40°. Remarkably, the filter response exhibits minimal sensitivity to both the incidence angle and the TE/TM polarization of the electromagnetic wave.

At 30 MHz, the transmission coefficient S_{21} is $-83\,dB$ for the angle of incidence $\theta = 0°$. Consequently, at low frequencies, this cell can be considered as an electromagnetic shield (see Figures 7 and 8).

3. DESIGN OF ANTENNA WITH MINIATURE FSS BASED REFLECTOR

For designing the antenna, the 5.9 GHz resonance frequency and the FR-4 substrate material are firstly selected. A lossy FR-4 substrate with dimensions ($Ws \times Ls$), relative permittivity of 4.3 and thikness of $hs = 1.6\,mm$ is used in the antenna design. For both the hexagonal patch and the ground plane (dimensions $Wg \times Lg$), this becomes the copper material with Thickness $hg = 35\,\mu m$. Starting from a hexagonal patch constructed from a rectangular patch of dimensions $Wa \times La$, we construct a hexagonal patch of side Lh. A rectangular slot of dimensions $a \times b$ is optimized, in order to obtain the proposed antenna resonant at this frequency. Proposed antenna topology is shown in figures 9 and 10. Design

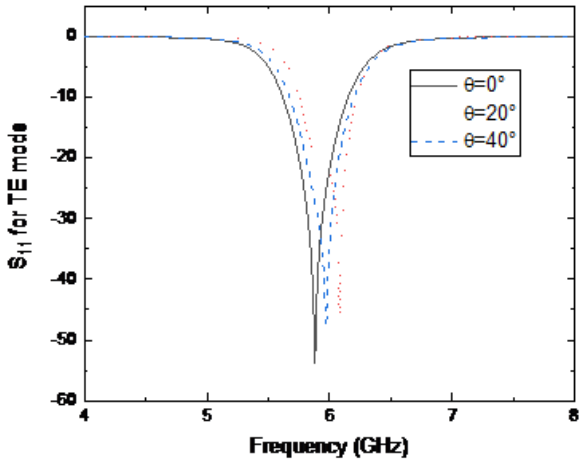

Figure 3: The reflection coefficient S_{11} of the FSS in TE mode for different angles of incidence.

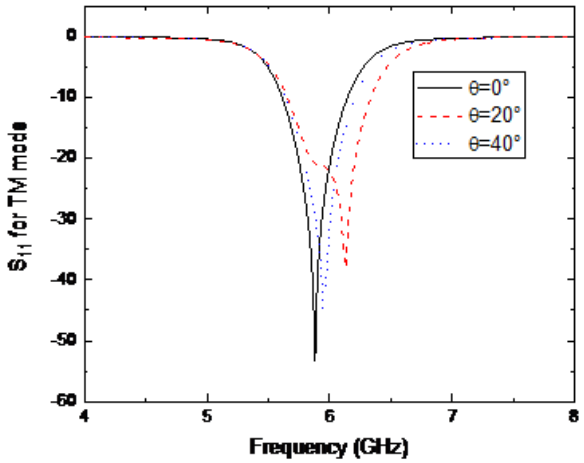

Figure 4: The reflection coefficient S_{11} of the FSS in TM mode for different angles of incidence.

Table 2
GEOMETRIC PARAMETERS OF THE PROPOSED NOTCHED HEXAGONAL ANTENNA OPTIMIZED AT 5.9 GHZ.

Parameters	La	Lh	Ws	Ls	Lg
Values (mm)	20	28.8	30	40	15.6
Parameters	Wg	Wf	Lf	a	
Values (mm)	30	3	17	2.8	

parameters are optimized to give performances at 5.9 GHz operating frequency and they are summarized in Table 2 in *mm*.

Figures 11 and 12 shows the radiation pattern of the hexagonal antenna alone at 5.9 GHz for $Phi = 0^{\circ}$ and 90°. The maximum gain is 3 dBi. The antenna radiates forward and backward.

In order to increase the gain of this antenna and direct its radiation forward, we propose the idea of placing a miniature metamaterial reflector behind the antenna and at a distance $d = \frac{\lambda}{4} = 12.7\,mm$, to

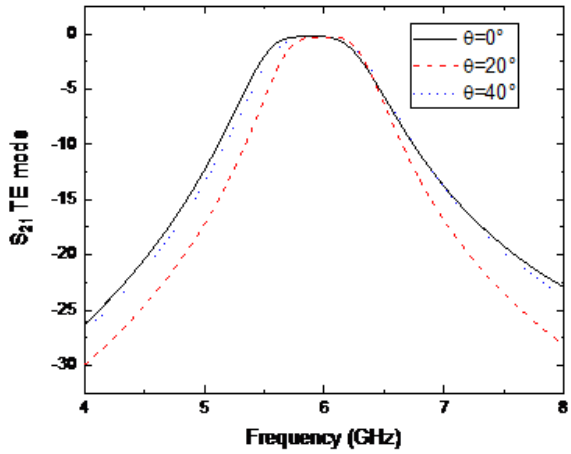

Figure 5: The transmission coefficient S_{21} of the FSS in TE mode for different angles of incidence.

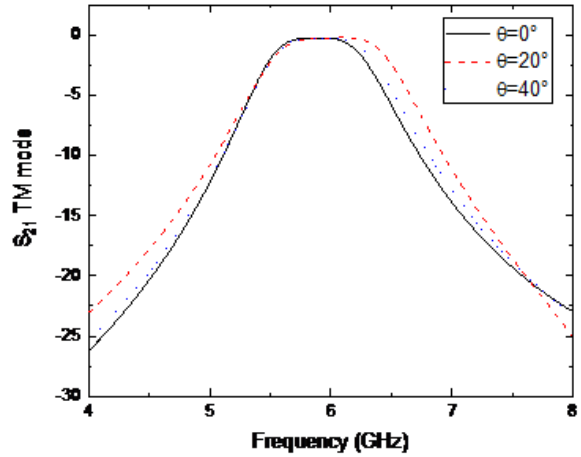

Figure 6: The transmission coefficient S_{21} of the FSS in TM mode for different angles of incidence.

Table 3
GEOMETRIC PARAMETERS OF THE PROPOSED FSS CELL OPTIMIZED AT 5.9 GHz.

Parameters	Rx	Ry	P	S
Values (mm)	10	10	0.4	0.7

achieve constructive interference with the primary source coming from this antenna. Figure 13 shows the shape of the proposed single-sided FSS-2 cell which plays the role of a reflector made up of 3×3 cells.

Figures 14 and 15 shows the 2D radiation pattern of the 3×3 FSS-2 reflector antenna at 5.9 GHz with an increase in gain to reach 7 dBi as well as the directivity.

4. INTEGRATED DESIGN OF METAMATERIAL FILTER AND ANTENNA WITH MINIATURE REFLECTOR

We will investigate the impact of the periodic structure with a period D shown in figures 1 and 2 on a closely located hexagonal antenna. Parameters such as S_{11}, radiation pattern, and antenna gain, both individually and with the FSS, will be analyzed. Figure 16 depicts a 5×7 array of second-order FSS cells

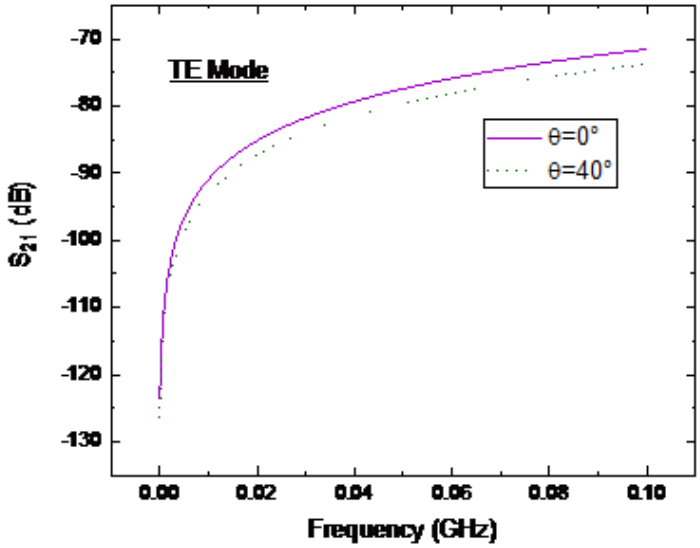

Figure 7: The transmission coefficient S_{21} of the FSS in TE mode in BF for different angles of incidence.

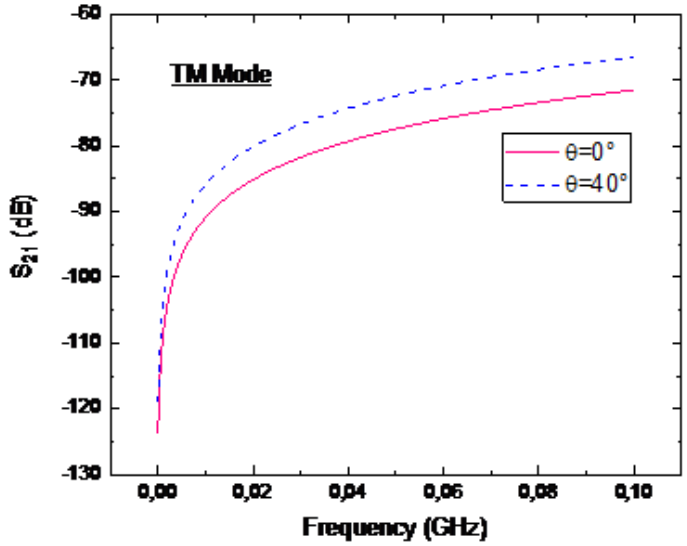

Figure 8: The transmission coefficient S_{21} of the FSS in TM mode in BF for different angles of incidence.

placed at a distance $e_1 = \frac{\lambda}{2}$ in the (Oz) direction above a vertical hexagonal monopole antenna with Reflector along the Oz axis. The same 5×7 array of second-order FSS cells is placed at a distance $e_2 = \frac{\lambda}{4}$ in cascade to obtain a selective filter.

Figure 17 illustrates the S_{11} parameter of the hexagonal antenna alone and in conjunction with a 5×7 array FSS cells. We note that the bandwidth of the antenna increases from $2.7\,GHz$ to $1.5\,GHz$ authorized by the filter of $[5 - 6.5]\,GHz$.

Figures 18 and 19 depict the gain as a function of θ at the frequency of $5.9\,GHz$ for $Phi = 0^\circ$ and 90°, respectively. It can be observed that the FSS impact significantly the radiation of the antenna by increasing gain and directivity. The antenna thus becomes more directive. At this frequency, the maximum gain of the antenna increases to $8\,dBi$ with an efficiency greater than 90% on the operating band.

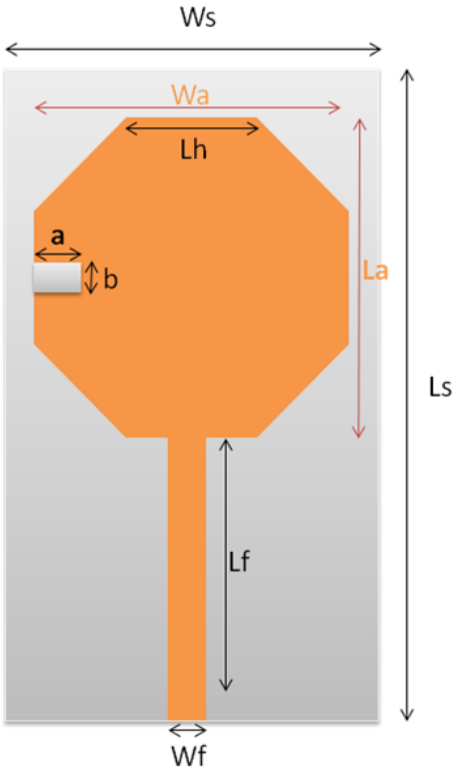

Figure 9: Antenna front side view.

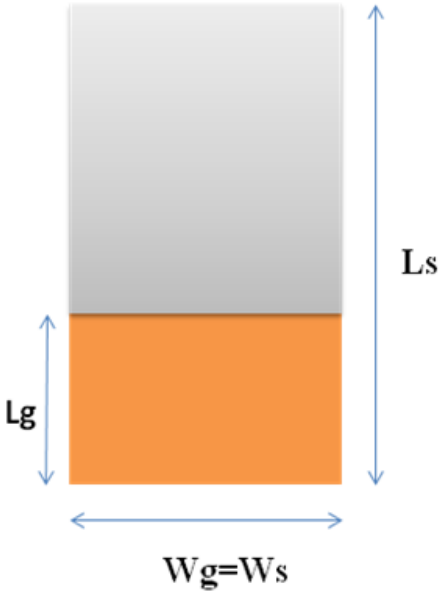

Figure 10: Antenna back side view.

5. Conclusion

In railway settings, the powerful signals used in train communication systems, especially in the lower frequency range, can disrupt the functioning of wireless devices by causing electromagnetic interference (EMI). To mitigate this issue, incorporating a filter onto the antenna can be highly advantageous. This paper proposes a filter-antenna design, utilizing a resonant metamaterial screen positioned near the

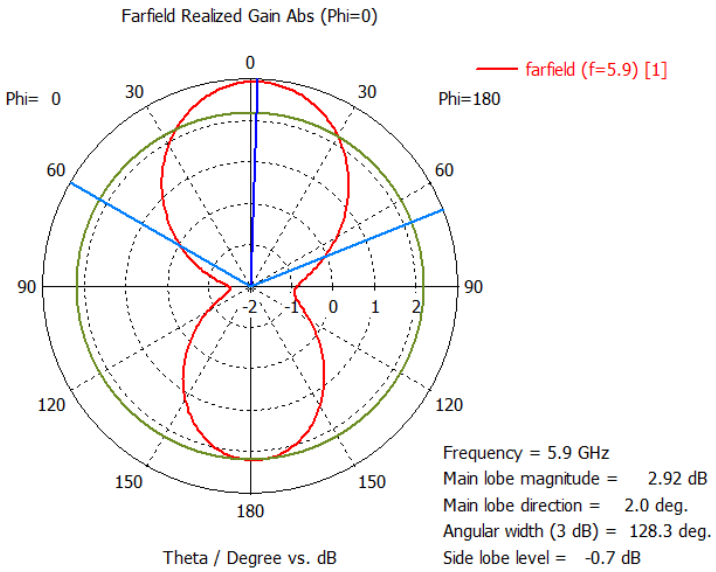

Figure 11: 2D radiation pattern of the hexagonal antenna alone at 5.9 GHz for $Phi = 0^{\circ}$.

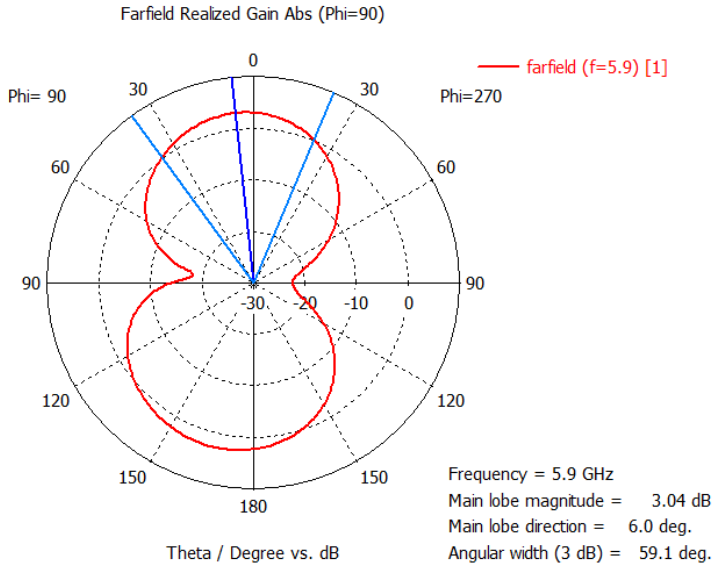

Figure 12: 2D radiation pattern of the hexagonal antenna alone at 5.9 GHz for $Phi = 90^{\circ}$.

patch element to maintain antenna performance at the 5.9 GHz operating frequency. Additionally, it offers out-of-band rejection with a minimum attenuation of 40 dB from 30 MHz to 1 GHz. Both numerical simulations and experimental tests successfully validate these results, positioning the design as a promising solution for EMI reduction in wireless railway applications. Furthermore, its simple design and single-layer construction suggest it can be fabricated at a low cost.

Declaration on Generative AI

The authors have not employed any Generative AI tools.

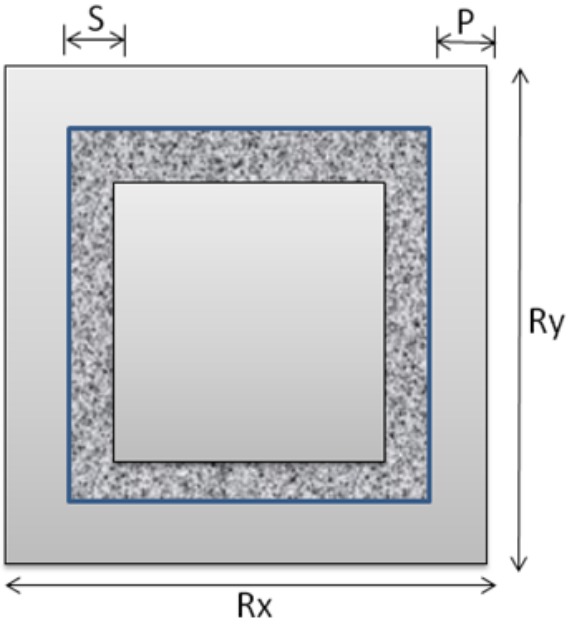

Figure 13: Shape of the FSS-2 cell of the reflector.

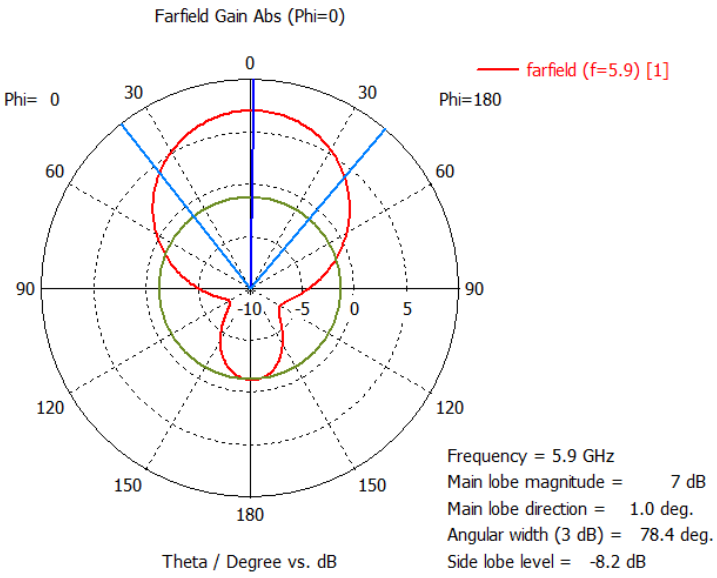

Figure 14: 2D radiation pattern of the hexagonal antenna with the 3×3 cells FSS-2 reflector at $5.9\,GHz$ for $Phi = 0^{\circ}$.

References

[1] B. A. Munk, Frequency Selective Surfaces: Theory and Design. New York: Wiley-Interscience, 2000.

[2] B. Lin, S. Du, H. Zhang, and X. Ye, "Design and Simulation of Frequency-Selective Radome Together with a Monopole Antenna," ACES JOURNAL, vol. 25, no. 7, pp. 620-625, (2010).

[3] K. Sarabandi and N. Behdad, "A frequency selective surface with miniaturized elements," IEEE Trans. Antennas Propag., vol. 55, no. 5, pp. 1239–1245, (2007).

[4] F. Bayatpur and K. Sarabandi, "Single-layer, high-order, miniaturized-element frequency selective surfaces," IEEE Trans. Microw. Theory Tech., vol. 56, issue 4, pp. 774-781, (2008).

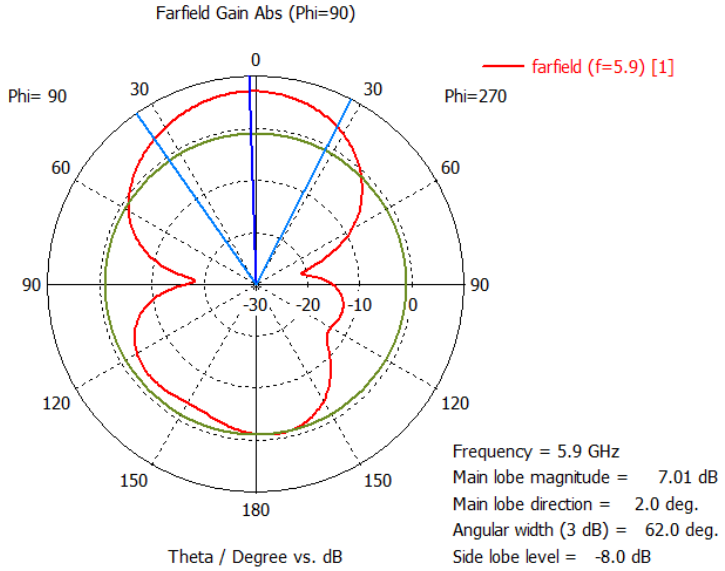

Figure 15: 2D radiation pattern of the hexagonal antenna with the 3×3 cells FSS-2 reflector at $5.9\,GHz$ for $Phi = 90^{\circ}$.

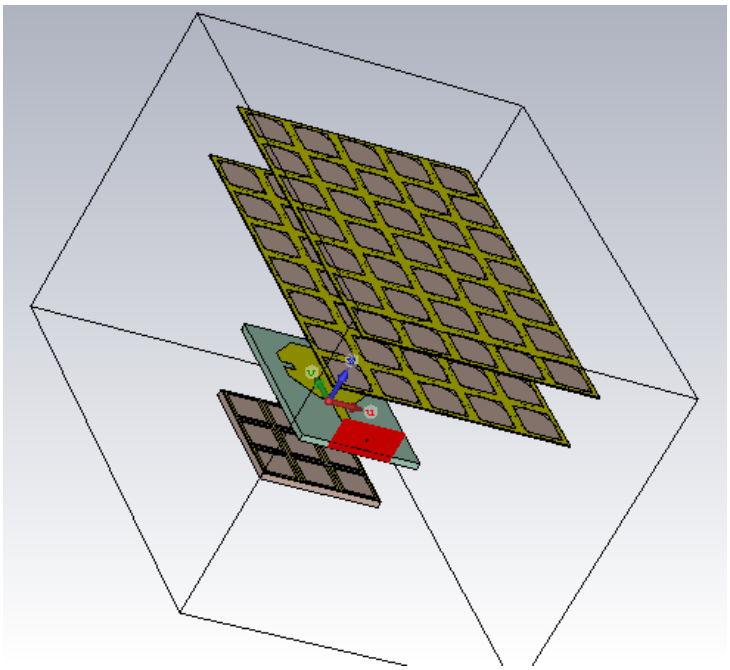

Figure 16: Hexagonal antenna shape with reflector and filter.

[5] F. Bayatpur, K. Sarabandi, "Multipole spatial filters using metamaterial based miniaturized-element frequency-selective surfaces," IEEE Trans. Microw. Theory Tech., vol. 56, issue 12, pp. 2742-2748, (2008).

[6] B. Lin, S. Zhou, X. Da, Y. Fang, Y. Li, and W. Li, "Compact miniaturised- element frequency selective surface," Electronics Letters, vol. 51, no. 12, pp. 883–884, (2015).

[7] F. Bayatpur and K. Sarabandi, "Miniaturized FSS and patch antenna array coupling for angle-independent, high-order spatial filtering," IEEE Microwave and Wireless Components Letters, vol. 20, no. 2, pp. 79–81, (2010).

[8] M. A. Al-Joumayly, and N. Behdad, "A generalized methode for synthesizing low-profile, band-pass frequency selective surfaces with non-resonant constituting elements," IEEE Trans. Antennas

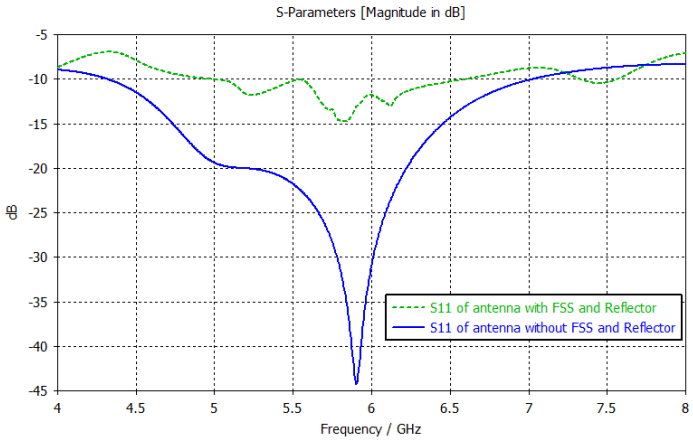

Figure 17: Reflection coefficient S_{11} of the hexagonal antenna with 3×3 cells reflector and the second order 5×7 cells FSS filter.

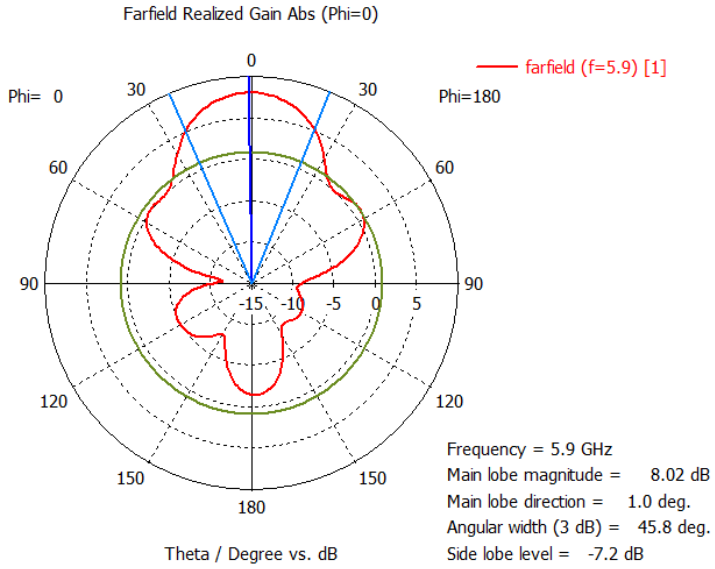

Figure 18: 2D radiation pattern of the hexagonal antenna with and without 5×7 FSS cells + 3×3 reflector cells at $5.9\,GHz$ for $Phi = 0^{\circ}$

.

Propag., vol. 58, no. 12, pp. 4033–4041, (2010).

[9] H. Zhou, S. Qu, B. Lin, J. Wang, H. Ma, Z. Xu, W. Peng, and P. Bai, "Filter-antenna consisting of conicol FSS radome and monopole antenna," IEEE Trans. Antennas Propag., vol. 60, no. 6, pp. 3040–3045, (2012).

[10] H., "Filter-antenna," IEEE Trans. Antennas Propag., vol. 60, no. 6, pp. 3040–3045, (2012).

[11] D. Minoli, K. Sohraby, and B. Occhiogrosso, "IoT considerations, requirements, and architectures for smart buildings: energy optimization and next-generation building management systems," IEEE Internet of Things Journal, vol. 4, no. 1, pp. 269-283, 2017.

[12] A. K. Arya, S. J. Kim, S. Park, D. H. Kim, R. S. Hassan, K. Ko, and S. Kim, "Shark-fin antenna for railway communications in LTE-R, LTE, and lower 5G frequency bands, " Progress In Electromagnetics Research, vol. 167, pp. 83-94, 2020.

[13] J. Cui, A. Zhang, and X. Chen, "An omnidirectional multiband antenna for railway application," IEEE Antennas and Wireless Propagation Letters, vol. 19, no. 1, pp. 54-58, 2020.

[14] A. K. Arya, S. J. Kim, and S. Kim, "A dual-band antenna for LTE-R and 5G lower frequency operations," Progress In Electromagnetics Research Letters, vol. 88, pp. 113-119, 2020.

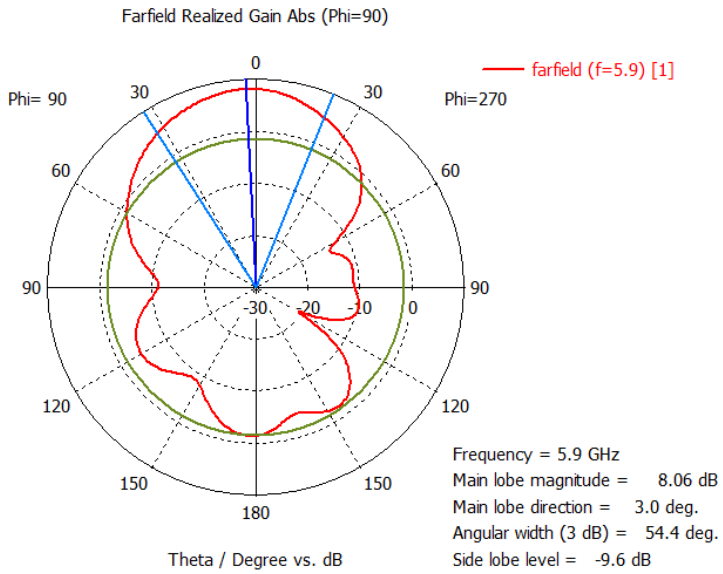

Figure 19: 2D radiation pattern of the hexagonal antenna with and without 5×7 FSS cells + 3×3 reflector cells at $5.9\,GHz$ for $Phi = 90^{\circ}$.

[15] J. Khan, S. Ullah, F. A. Tahir, F. Tubbal, and R. Raad, "A sub-6 GHz MIMO antenna array for 5G wireless terminals," Electronics, vol. 10, no. 24, article no. 3062, 2021.

[16] A. K. Arya, S. Kim, K. Ko, and S. Kim, "Antenna for IOT-based future advanced (5G) railway communication with end-fire radiation," IEEE Internet of Things Journal, vol. 9, no. 9, pp. 7036-7042, 2022.

[17]] M. Alibakhshikenari, F. Babaein, B.S. Virdee, S. Aissa, E. Limiti, et al., A comprehensive survey on ‘‘Various decoupling mechanisms with focus on metamaterial and metasurface principles applicable to SAR and MIMO antenna systems, IEEE Access 8 (2020) 192965–193004.

[18]] W. Wang, Z. Fang, K. Tang, X. Wang, Z. Shu, Z. Zhao, Y. Zheng, Wideband gain enhancement of MIMO antenna and its application in FMCW radar sensor integrated with CMOS-based transceiver chip for human respiratory monitoring, IEEE Trans. Antenn. Propag. 71 (1) (2022) 318–329.

[19]] J.-N. Lee, S.B. Hyun, Y.K. Cho, A compact ultra-wideband chip antenna with bandwidth extension patch and simple isolator for mimo systems for mobile handheld terminals, Journal of Electromagnetic Engineering and Science 22 (3) (2022) 272–282.

[20]] R. Yang, Sh Xi, Q. Cai, Z. Chen, X. Wang, C. Liu, A compact planar dual-band multiple-input and multiple-output antenna with high isolation for 5G and 4G applications, Micromachines 12 (2021) 1–8.

[21]] J. Zhang, C. Du, R. Wang, Design of a four-port flexible UWB-MIMO antenna with high isolation for wearable and IoT applications,", Micromachines 13 (12) (2022) 2141.

[22]] B. Zhang, J.M. Jornet, I.F. Akyildiz, Z.P. Wu, Mutual coupling reduction for ultra-dense multi-band plasmonic nano-antenna arrays using graphene-based frequency selective surface, IEEE Access 7 (2019) 33214–33225.

[23]] M.A. Sufian, N. Hussain, A. Abbas, J. Lee, S.G. Park, N. Kim, Mutual coupling reduction of a circularly polarized MIMO antenna using parasitic elements and DGS for V2X communications, IEEE Access 10 (2022) 56388–56400.

[24]] A. Abbas, N. Hussain, M.A. Sufian, J. Jung, S.M. Park, N. Kim, Isolation and gain improvement of a rectangular notch UWB-MIMO antenna, Sensors 22 (4) (2022) 1–14.

[25]] M. Fallgren, M. Dillinger, T. Mahmoodi, T. Svensson, J. Wiley, Cellular V2X for Connected Automated Driving, vol. 270, Wiley Online Library, 2021.